Journal of ELECTRONIC MATERIALS, Vol. 36, No. 11, 2007
DOI: 10.1007/s11664-007-0222-5

*Special Issue Paper*

# Substrate Dissolution and Shear Properties of the Joints between Bi-Ag Alloys and Cu Substrates for High-Temperature Soldering Applications

JENN-MING SONG,[1,2] HSIN-YI CHUANG,[1] and ZONG-MOU WU[1]

1.—Department of Materials Science and Engineering, National Dong Hwa University, Hualien 974, Taiwan. 2.—e-mail: samsong@mail.ndhu.edu.tw

The present study investigated interfacial reactions between Cu substrates and Bi-Ag alloys during soldering. Without forming intermetallic compounds (IMCs), the molten solder grooved and further penetrated along the grain boundaries (GBs) of the Cu substrate. An increase in Ag content enhanced GB grooving, raised the dissolution rate and also the amount of dissolved Cu in molten Bi. A stoichiometric Cu-Bi phase formed isothermally in liquid solders and considerably affected the Cu dissolution kinetics. The results also show that Bi-Ag/Cu joints possessed a better shear strength than the Pb-Sn/Cu, which implies that mechanical bonding by grain-boundary grooves was strong enough to withstand shear deformation.

**Key words:** High-temperature Pb-free solders, Bi-Ag, substrate dissolution, shear strength

## INTRODUCTION

Due to environmental concerns, the use of Pb will soon be banned in the electronic packaging industry. Hence the search for lead-free solders has recently become an important issue. The Pb-free replacement solders for eutectic Sn-Pb, such as Sn-Ag-Cu and Sn-Zn, have been well studied. However, the development of high-temperature Pb-free solders to replace conventional high-Pb alloys, for example Pb-3–5Sn, is still in its infancy. A high-Pb solder should have a solidus higher than 260°C, so that the solder is capable of surviving secondary reflow at 250°C. The liquidus also needs to be lower than 400°C due to the limitation of the glass-transition temperature of the polymeric substrate.[1] Among the proposed alloy systems, their proper eutectic temperature of 262.5°C makes the Bi-Ag alloys with a eutectic composition of Bi-2.5wt.%Ag a promising replacement.[1–3] However, the development of this solder alloy system is still ongoing, mainly due to its inferior thermal and electrical conductivity as well as poor workability. It has recently been demonstrated that increasing the Ag content of Bi-Ag to 11 wt.% promotes an increase in thermal conductivity[2] and ductility.[4]

Copper is the most common electronic substrate. A recent report indicated that grooves which appeared at the intersections of Cu grain boundaries with the Bi-Ag/Cu interface were believed to provide mechanical bonding for Bi-Ag/Cu joints.[5] To gain deeper insight into this solder system, quantitative investigation of the interaction between the Cu substrate and Bi-Ag alloys during soldering, as well as the shear performance of the joints, was performed in this study.

## EXPERIMENTAL PROCEDURES

The solder alloys used were eutectic Bi-2.5Ag and hypereutectic Bi-11Ag. Pure Bi was also prepared for comparison. As shown in Fig. 1, 5 g of the solder was placed in a quartz tube with a 5 mm inner diameter and then soaked in a salt bath at a fixed temperature. The Cu wire specimens (annealed 99.9% pure Cu) of 1 mm in diameter were sequentially degreased in NaOH solution, deoxidized in $HNO_3$ and dipped in a dimethylammonium chloride

---

(Received March 11, 2007; accepted July 23, 2007;

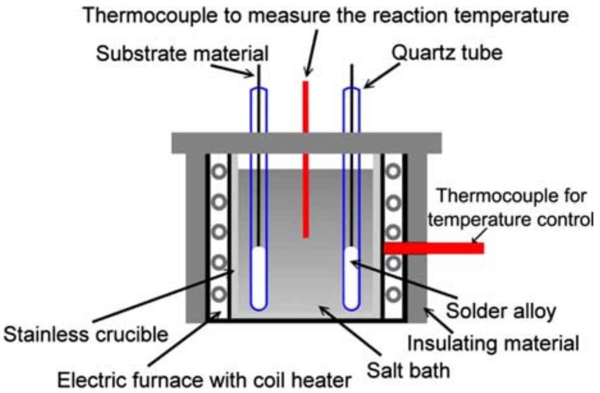

Fig. 1. Schematic diagram of the apparatus for substrate dissolution test.

(DMAHCl) solution prior to testing. The fluxed specimen was soaked in the molten solder for the desired duration. The immersion depth of the Cu wires into the solder was 30 mm. The soaking temperatures were kept constant at 350, 380, and 410°C to study the reaction kinetics. After a certain holding time, the tube was quenched in water. The residual diameter of the wires was determined from the residual cross-sectional area of the Cu wires 15 mm from the lower end. Each datum was the average of three samples.

Single-lap specimens, as shown schematically in Fig. 2, were used to investigate the shear properties. Pb-5wt.%Sn joints were also prepared for comparison. A stainless-steel clamping apparatus was used to fix two rods with a diameter of 3 mm. The gap between the adjacent ends of the rods was adjusted to be 0.3 mm. The rinsing and fluxing procedures are shown above. A soldering tape was also applied to prevent undesired reactions. The clamped rods were sequentially dipped into a solder bath (350°C for 1 min) to produce a 0.3-mm-thick solder joint. The cooling rate after soldering was estimated to be about 8.6°C/s. The shear tests were carried out with the strain rate of 0.003 $s^{-1}$. Each datum was the average of more than five measurements.

Microstructural characteristics of the specimens were investigated by scanning electron microscopy (SEM) and electron probe microanalysis (EPMA) equipped with wavelength-dispersive spectrometers (WDS).

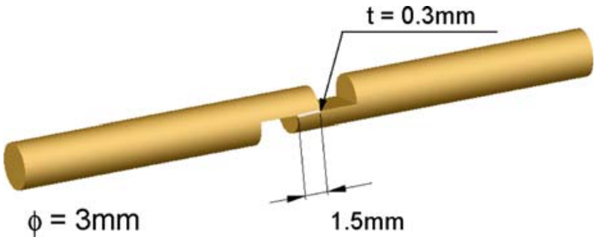

Fig. 2. The dimensions of the single-lap specimens.

## RESULTS

### Dissolution of Cu in Liquid Bi-Based Solders

The decrease in the radius of the Cu wires as a function of the square root of the reaction time is plotted in Fig. 3. According to the results, the radius reduction first followed a parabolic relationship with reaction time under all conditions (referred to as the parabolic stage hereafter). Afterwards, the amount of dissolution remained almost constant (referred to as the steady stage), which usually implies that the solubility limit of Cu in the liquid solder has been reached. Take the dissolution data at 350°C as an example example (Fig. 3a); the slope of the dissolution curve was drastically diminished with the reaction time of 20 min for pure Bi and Bi-2.5Ag. Interestingly, in the case of Bi-11Ag the time for the slope change was prolonged to 40 min. The same tendency could be observed at all the soaking temperatures.

For comparison, Tables I and II list the dissolution rate of Cu in the first 10 min and the Cu concentration in the liquid solders in the steady stage, which were calculated by dividing the Cu weight loss (estimated from the radius reduction) into the solder weight, at different temperatures. These results indicate that either a higher Ag content or a higher reaction temperature result in faster substrate dissolution. Similarly, the amount of dissolved Cu and consequent Cu concentration in molten solders increased in turn from pure Bi, Bi-2.5Ag to Bi-11Ag. Accordingly, it can be seen that the solubility of Cu in Bi could be increased by adding Ag and raising the reaction temperature.

Moreover, the natural logarithm of the dissolution rate against the reciprocal reaction time in the first 10 min of the parabolic stage is plotted in Fig. 4. The quotient of the straight slope and gas constant represents the activation energy of dissolution. The activation energies for Cu dissolution into the Bi-based solders investigated are very close: 17.14 kJ/mol for pure Bi, 17.76 kJ/mol for Bi-2.5Ag, and 16.59 kJ/mol for Bi-11Ag, suggesting the same dominant mechanism for Cu dissolution.

### Microstructural Evolution During Long-Time Soaking

Figure 5 illustrates the interfacial morphologies of the Cu wires after soaking in liquid Bi and Bi-Ag respectively, which show that instead of forming IMC layers, GB grooving occurred at the solder/substrate interface. Also, some gray particles or needles of the newborn phase, indicated by the arrows, could be observed within the solder in addition to Bi and Ag. The magnified structure in Fig. 6a and b reveal that GB grooves appeared at pure Bi/Cu and Bi-11Ag/Cu after a short period of soaking at 350°C for 10 min. A higher temperature and extended reaction period resulted in a greater degree of grooving and even GB penetration, as

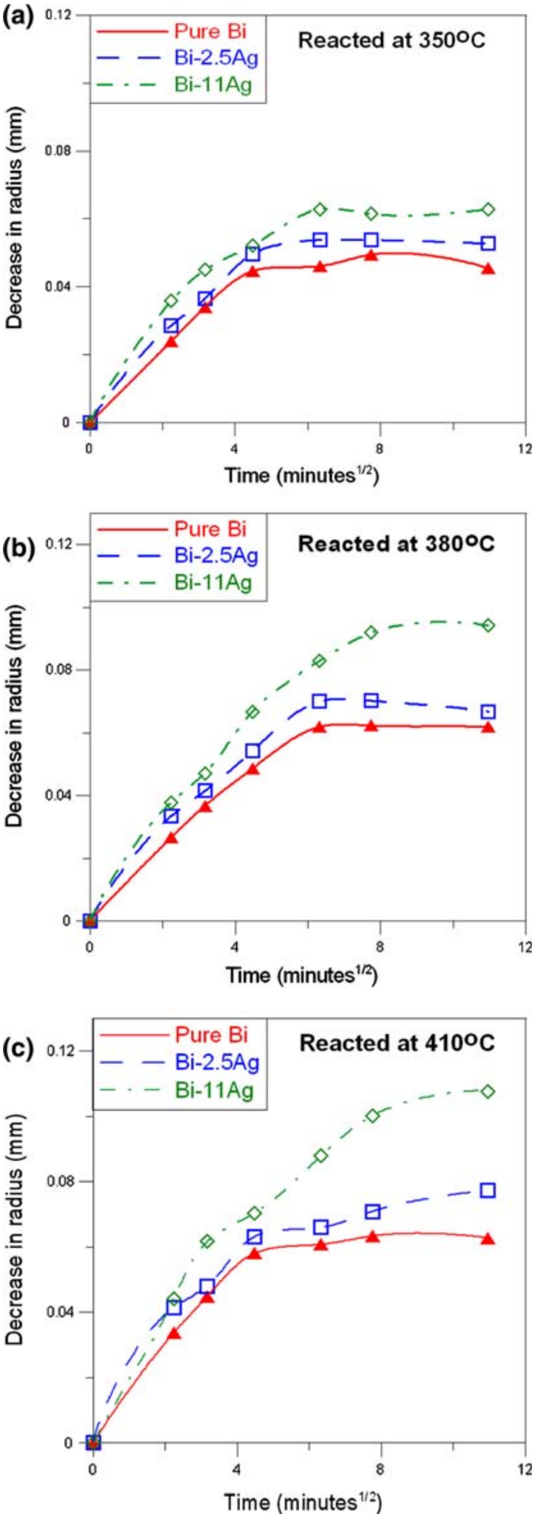

Fig. 3. The decrease in radius of Cu against the square root of time at: (a) 350°C, (b) 380°C, and (c) 410°C; the initial radius of the Cu wires is 0.5 mm.

**Table I. Dissolution Rate of Cu in Molten Solder During the First 10 min of the Reaction**

| Temp./ Alloy (°C) | Dissolution Rate (μm/min) | | |
|---|---|---|---|
| | Pure Bi | Bi-2.5Ag | Bi-11Ag |
| 350 | 3.7 | 4.1 | 5.0 |
| 380 | 4.0 | 4.7 | 5.3 |
| 410 | 4.9 | 5.5 | 6.7 |

**Table II. Concentration of Dissolved Cu in Liquid Solder in Comparison with the Theoretical Cu Solubility**

| Temp./ Alloy (°C) | Amount of Dissolved Cu in the Solders (wt.%) | | | |
|---|---|---|---|---|
| | Bi (Ref.) | Pure Bi | Bi-2.5Ag | Bi-11Ag |
| 350 | 0.28 | 0.70 | 0.81 | 0.95 |
| 380 | 0.41 | 0.94 | 1.01 | 1.38 |
| 410 | 0.60 | 0.95 | 1.16 | 1.56 |

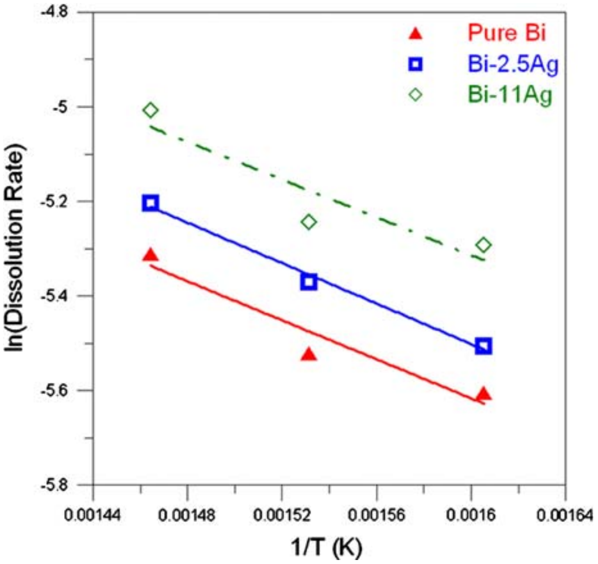

Fig. 4. The natural logarithm of the dissolution rate against the reciprocal reaction temperatures.

shown in Fig. 6c and d. The depth of GB grooves after 120 min reaction were measured and are listed in Table III, which shows that either Ag additions or an increased reaction temperature accelerate the GB grooving of Cu by liquid Bi.

New phases resulting from the reaction of dissolved Cu and liquid solders are illustrated in Fig. 7. In the case of pure Bi, Fig. 7a and b, acicular Cu-Bi phase with the composition of 59.6at.%Cu-40.4at.%Bi gathered with a fanlike appearance. Interestingly, in the Ag containing solders, Fig. 7c and d, the Cu-Bi phase exhibited a round appearance and contained a certain amount of Ag (the composi-

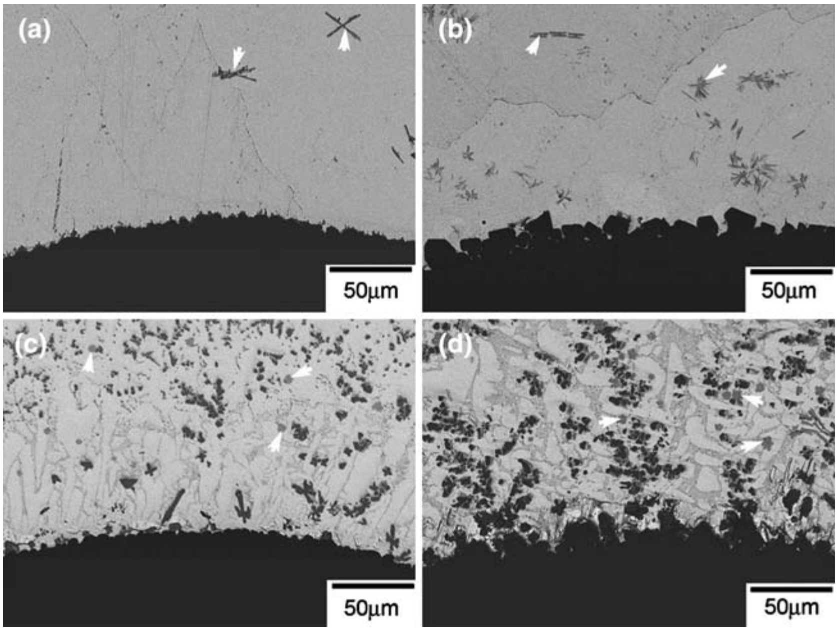

Fig. 5. Microstructure in the vicinity at the interface of Bi/Cu: (a) 350°C for 120 min, and (b) 410°C for 120 min; and Bi-11Ag/Cu: (c) 350°C for 120 min, and (d) 410°C for 120 min (the gray newborn phase is indicated by the arrows).

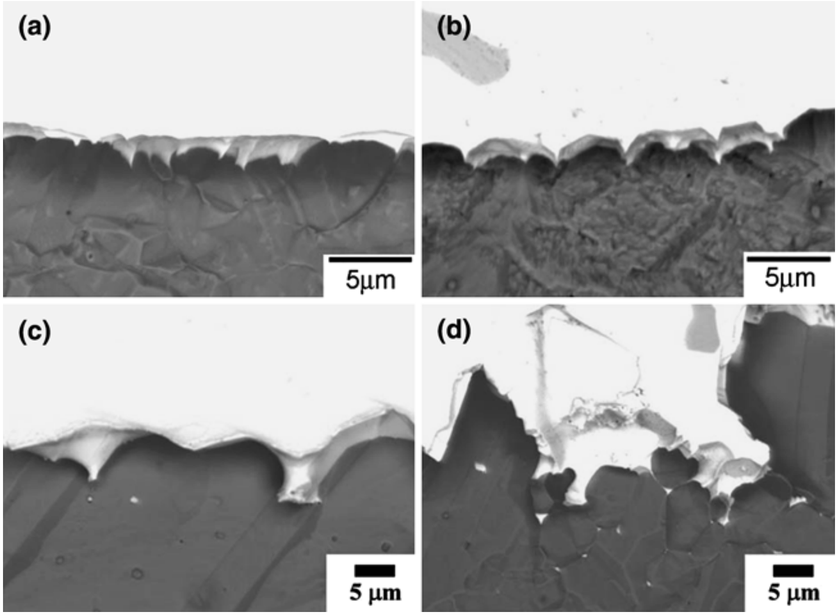

Fig. 6. Interfacial morphologies of the samples after reaction under different conditions: (a) pure Bi/Cu at 350°C for 10 min, (b) Bi-11Ag/Cu at 350°C for 10 min, (c) pure Bi/Cu at 410°C for 120 min, and (d) Bi-11Ag/Cu at 410°C for 120 min.

tion was 56.3 at%Cu-39.2at.%Bi-4.5at.%Ag). By way of comparison, Fig. 7a and c reveal that the amount of Cu-Bi phase in Bi-11Ag solder was larger than that in pure Bi.

## Shear Strength and Fracture Surface of Joints

Figure 8 shows the shear strength of the joints after 1 min of soldering at 350°C. The average joint shear strength in decreasing order was Bi-11Ag/Cu, Bi-2.5Ag/Cu, and then Pb-5Sn/Cu. Although the strength of the Bi-Ag/Cu samples was greater than the Pb-5Sn/Cu samples, the data were spread over a wider range. In addition, the fracture surfaces of the three joint samples, Fig. 9, reveal that fracturing almost occurred within the solder. The fracture surface of the Pb-5Sn/Cu was more rugged than those of the Bi-Ag/Cu. There were no interfacial reaction layers or Cu substrate exposed.

**Table III. The Grooving Depth Measured as the Reaction Time Reached 120 Min ($\mu$m)**

| Temperature/Alloy (°C) | Pure Bi | Bi-11Ag |
|---|---|---|
| 350 | 2.02 | 3.17 |
| 380 | 2.05 | 3.28 |
| 410 | 7.70 | 8.97 |

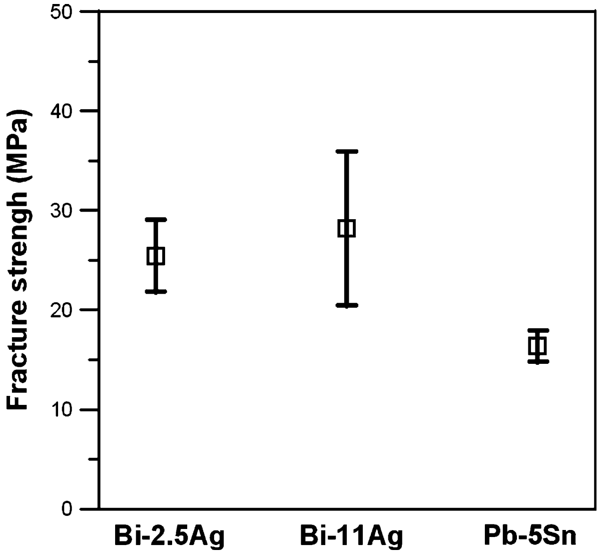

Fig. 8. Fractured shear strength of Bi-Ag/Cu and Pb-5Sn/Cu joints.

## DISCUSSION

Based on the binary Bi-Cu phase diagram,[6] the theoretical solubility of Cu in liquid Bi was estimated to be about 0.28 wt.% at 350°C, 0.41 wt.% at 380°C and 0.6 wt.% at 410°C. However, the above results show that the amounts of dissolved Cu in both pure Bi and Bi-Ag liquids at these temperatures were much higher. According to Dybkov analysis of the kinetics of dissolution of a solid in a liquid,[7] the dissolution of substrate into the solder liquid can be expressed as

$$\frac{\mathrm{d}c}{\mathrm{d}t} = k\frac{S}{V}(c_\mathrm{s} - c) \qquad (1)$$

where $c_\mathrm{s}$ = the solubility limit of substrate element in the liquid at the reaction temperature, $c$ = concentration of the substrate, $k$ = dissolution rate constant, $S$ = surface area of the substrate, and $V$ = volume of the liquid. When $c = c_\mathrm{s}$, the rate of substrate atoms going into the liquid is equal to the rate of atoms leaving the liquid for the substrate. That brings about a termination of the dissolution reaction because a dynamic equilibrium is held between the substrate and the liquid. However, the dissolution data in this study show that the radii of the substrate proceeded to reduce even when the dissolved amount exceeded the theoretical value, which implies that the dynamic equilibrium no longer existed. In order to explain this unusual behavior, the phenomena observed, including GB grooving and the formation of Cu-Bi phase, should be clarified.

Grain-boundary grooving and even penetration were demonstrated to occur at Bi/Cu and Bi-Ag/Cu

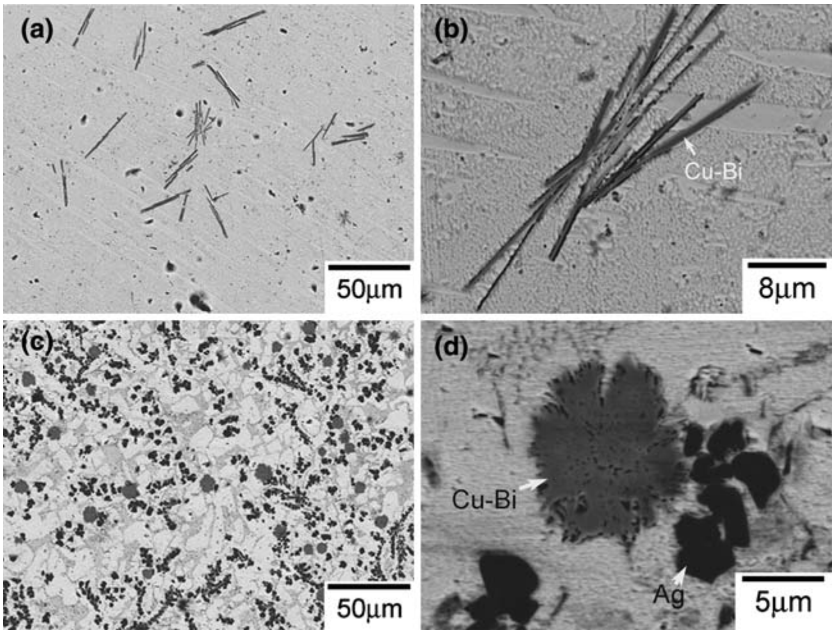

Fig. 7. Micrographs of pure Bi and Bi-11Ag samples after reaction with Cu at 380°C for 120 min: (a and b) pure Bi and (c and d) Bi-11Ag.

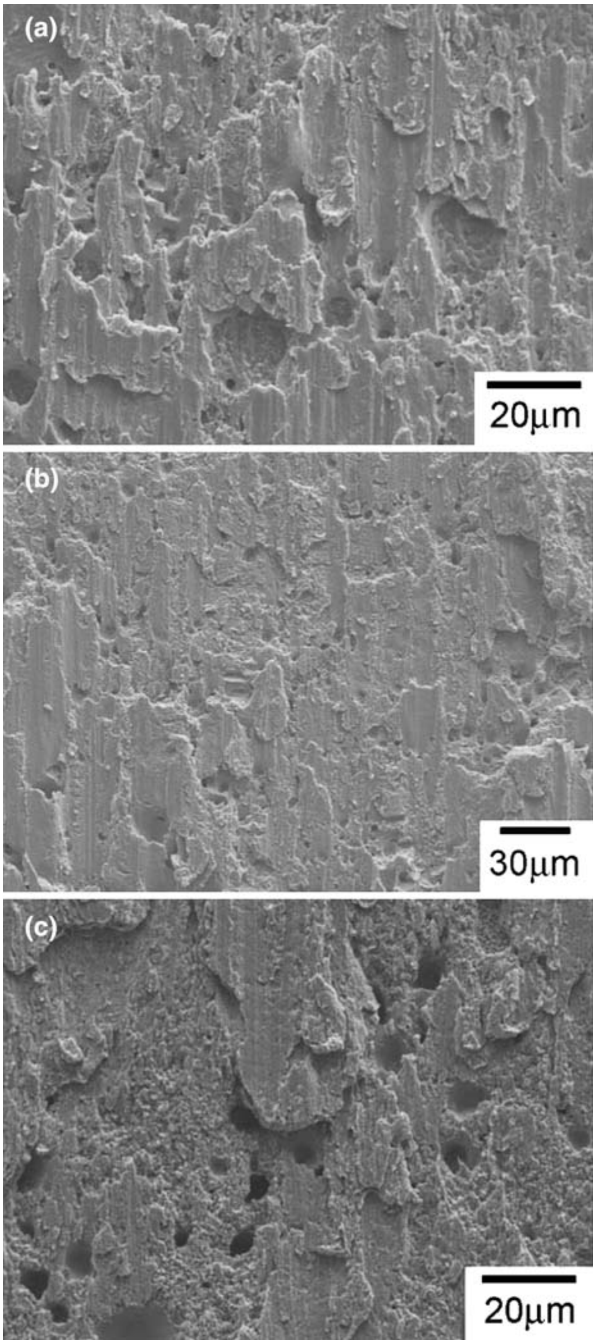

Fig. 9. Fracture surface after shear deformation: (a) Bi-2.5Ag, (b) Bi-11Ag, and (c) Pb-5Sn.

interfaces at soldering temperatures ranging from 350°C to 410°C. The addition of Ag to liquid Bi and a higher reaction temperature enhanced the GB grooving behavior, which was strongly positively correlated with the trend in the dissolution. This implies that dissolution at GBs plays an important role in the interfacial reaction between Cu and liquid Bi.

There are two mechanisms causing grain-boundary grooves;[8,9] the effect of surface tension when the grain boundary energy ($\gamma_{GB}$) is more than two times the solid–liquid interfacial energy ($\gamma_{SL}$), and the greater dissolution rate at grain boundaries (grooving rate) compared to flat surfaces. Joseph et al. reported that no groove was observed along the grain boundary when immersing Cu in pure Bi melt. Conversely, Cu GB grooving occurs when the liquid Bi contains a certain amount of Cu because the grooving rate at grain boundaries would be larger than the dissolution rate at the flat surface due to the reduced solute concentration gradient in the liquid.

In this study, GB grooving could be observed after only a short period of soaking, as seen in Fig. 6a and b. The whole process can be described schematically in Fig. 10. In the beginning, Cu atoms from both the GBs and surface dissolved into molten Bi or Bi-Ag alloys, Fig. 10a. Consequently, grooves started to form at the GBs due to the reduced $c_s$–$c$ value. When the solubility limit was reached, Fig. 10b, the Cu-Bi phase precipitated and consumed Cu in the liquid to some extent. Thus, the dissolution reaction could still proceed. The parabolic kinetics suggesting the diffusion control mechanism usually occurs in the case of the reaction coupling with interfacial IMC layer. Since there was no IMC formed at the interface between Bi solders and Cu, it can deduced that the dissolution process except for the very early stage was controlled by the growth of Cu-Bi phase and how fast it consumed Cu. The slope change in the dissolution curves from the parabolic stage to steady stage may be ascribed to the GB penetration and thus tunneling. As illustrated in Fig. 10c, molten Bi continued to penetrate along the Cu grain boundaries and give rose to tunneling, deep and spread into the Cu substrate, Fig. 6d. Those tunnels are more-rapid dissolution paths and provided a great amount of Cu atoms. Therefore, no more Cu dissolved from the flat surface and thus the external diameter of the Cu wires remained almost constant. This implies that the dissolved amount of Cu was still underestimated in Table II.

As already noted above, needle-like Cu-Bi and spherical Cu-Bi-Ag formed, respectively, within the pure Bi and Bi-Ag melts during soaking. The composition had a stoichiometric Cu/Bi ratio of about 3/2 according to the WDS analytical results. Actually, there is no such phase in the binary Cu-Bi phase diagram. It is likely to be a metastable phase found by Covington et al.,[10] which forms through precipitation from liquid Bi supersaturated with Cu. For comparison, a Bi-11Ag-5Cu sample was prepared through solidification from a temperature above 600°C, of which the continuous cooling curve and the microstructure were shown in Fig. 11. As illustrated, the Cu rich phase was identified as the primary Cu in the solidified structure, rather than the Cu-Bi phase in the isothermally processed samples shown in Fig. 7. Accordingly, it can be inferred that the Cu-Bi phase was an isothermal reaction product. Covington suggested that this compound could not be regarded as stable phase since it can be

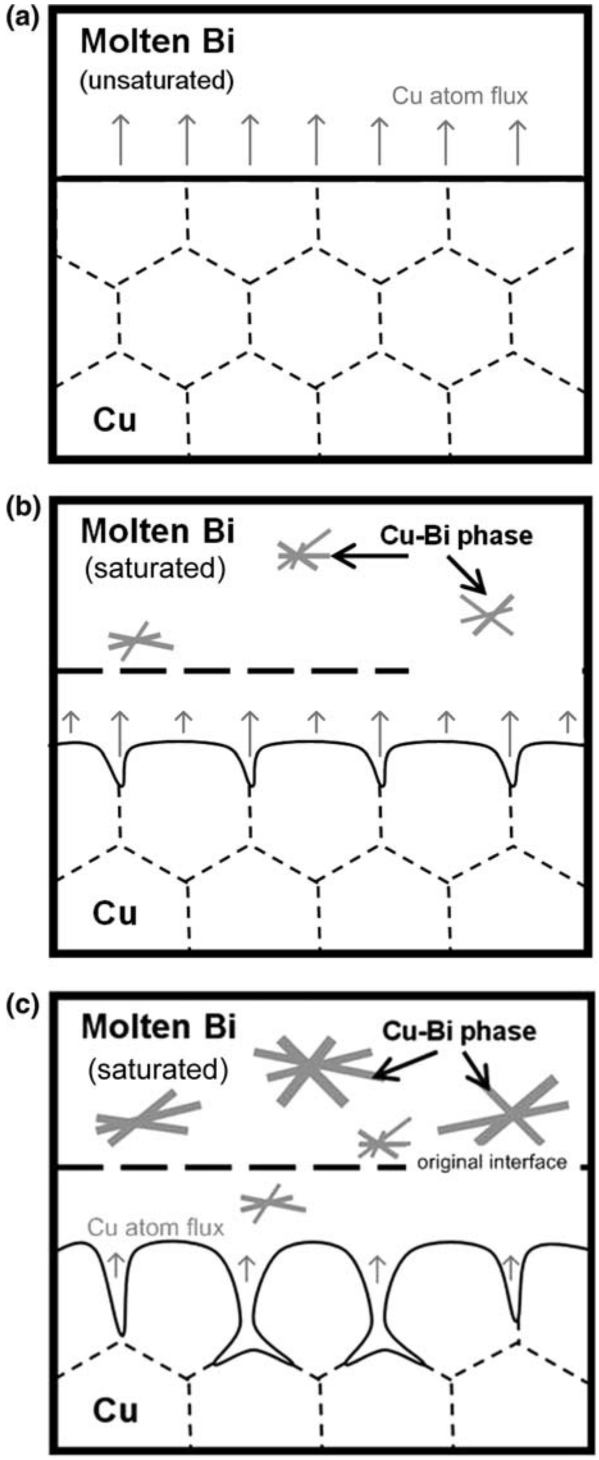

Fig. 10. Schematic descriptions of the relationship between the dissolution behavior and the microstructural change within the molten solder during soaking: (a) the initial stage, (b) the parabolic stage, and (c) the steady stage.

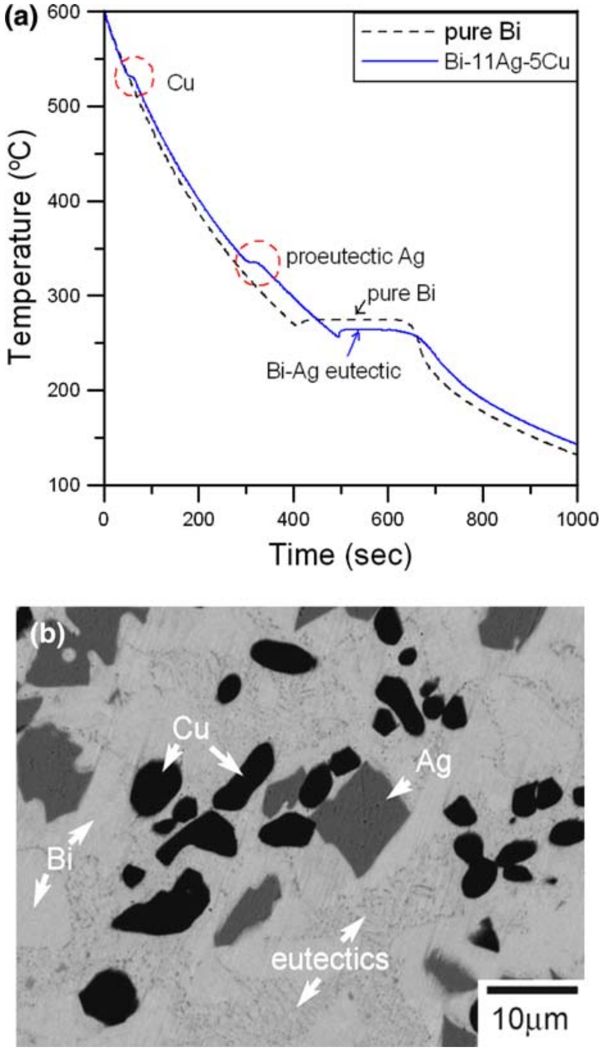

Fig. 11. (a) Cooling curves of pure Bi and Bi-11Ag-5Cu alloys, (b) the microstructure of the Bi-11Ag-5Cu alloy solidified under the cooling condition in (a).

produced only by precipitation from Bi supersaturated with Cu in the absence of Cu nuclei. Thus we can consider that in the isothermal liquid Bi without Cu nuclei, Cu-Bi phase forms preferentially (Fig. 12). If Cu nuclei are present, the Cu atoms will deposit on them to form the stable phase, Cu, in preference to forming the Cu-Bi compound. The Cu-Bi phase still deserves to pay attention, since it significantly influences the Cu substrate dissolution process and furthermore, it will remain and grow in the structure after high temperature storage at 150°C instead of decomposition.[11] However, very little is know about this phase at this juncture and further comment will be reserved until additional investigations are completed.

In the case of Cu dissolved in liquid Bi-Ag, it was found that a small portion of Cu was substituted by Ag and the shape of Cu-Bi phase became round. Most importantly, the amount of the Ag containing Cu-Bi precipitates was larger than for Cu-Bi in liquid Bi. Therefore, it can be inferred that Ag enhanced the formation of Cu-Bi, resulting in a reduced Cu concentration in liquid, which may have been responsible for the greater quantity and speed

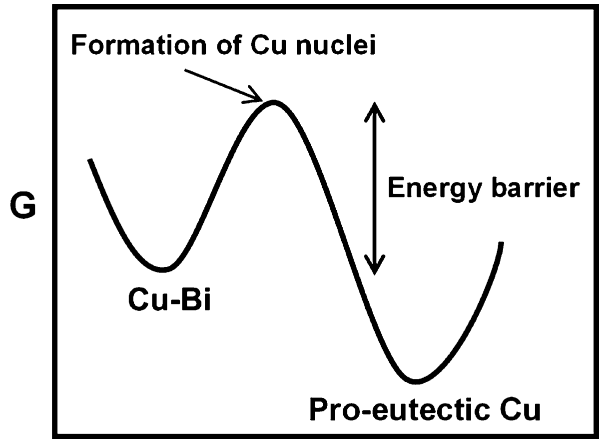

Fig. 12. Schematic sketch (not to scale) of the relationship between the Cu-rich phases in the Cu-Bi system and the corresponding Gibb's free energy.

of Cu dissolution as well as the prolonged parabolic stage.

Regarding the shear tests, it can be noted that the properties of the bulk solder dominate the shear strength since the whole fracturing path was within the solder instead of interface. The greater shear strength of Bi-Ag/Cu joints could be ascribed to the higher deformation resistance of Bi-Ag alloys according to Lalena's report,[1] revealing that the ultimate tensile strength of Bi-11Ag is 59 MPa and that for Pb-5Sn is 25 MPa.

## CONCLUSIONS

In liquid Bi-Ag, the dissolution of Cu substrate was accelerated and Cu solubility enhanced by an increased Ag content and a higher reaction temperature. It is worth noting that the dissolution process was found to be significantly affected by two specific phenomena: grooving along Cu grain boundaries and the formation of Cu-Bi phase. The release of Cu resulting from GB grooving plays an important role in the Cu dissolution, especially when the dissolved amount of Cu in the liquid solders exceeded the theoretical Cu solubility limit. Stoichiometric Cu-Bi, which precipitated isothermally from the liquid solders saturated with Cu, depleted the Cu concentration in the liquid and thus allowed the Cu dissolution to proceed. The results of single-lap shear tests indicated that Bi-Ag/Cu joints possessed a greater shear strength than the Pb-Sn/Cu. This suggests that grain boundary grooves at the Bi-Ag/Cu interface could provide firm mechanical bonding, and the shear strength depended on the deformation resistance of bulk solders rather than the form of interfacial bonding.

## ACKNOWLEDGEMENT

This work is supported by the National Science Council of R.O.C. (Contract: NSC 95-2221-E-259-014), for which the authors are grateful.

## REFERENCES

1. L.N. Lalena, N.F. Dean, and M.W. Weiser, *J. Electron. Mater.* 31, 1244 (2002).
2. J.H. Kim, S.W. Jeong, and H.M. Lee, *Mater. Trans.* 43, 1873 (2002).
3. M. Rettenmayr, P. Lambracht, B. Kempf, and M. Graff, *Adv. Eng. Mater.* 7, 965 (2005).
4. J.M. Song, H.Y. Chuang, and T.X. Wen, *Metall. Mater. Trans.* A 38, 1371 (2007).
5. J.M. Song, H.Y. Chuang, and Z.M. Wu, *J. Electron. Mater.* 35, 1041 (2006).
6. T.B. Massalski, ed., *Binary Alloy Phase Diagrams*, 2nd ed. (Materials Park, OH: ASM International, 1992), vol. 1, pp. 732–733.
7. V.I. Dybkov, *J. Mater. Sci.* 28, 6371 (1993).
8. B. Straumal, T. Muschik, W. Gust, and B. Predel, *Acta Metall. Mater.* 40, 939 (1992).
9. B. Joseph, F. Barbier, G. Dagoury, and M. Aucouturier, *Scripta Mater.* 39, 775 (1998).
10. A.K. Covington, K. Groenwolt, and B.W. Howlett, *J. Inst. Met.* 89, 291 (1960–61).
11. J.M. Song, K.K. Lew, and H.Y. Chuang (136th TMS Meeting, 27, February 2007).